

## Dual Role of Purification and Functionalisation of Single Walled CNT by Electron Cyclotron Resonance (ECR) Nitrogen Plasma\*

Ganjigunte R. S. Iyer,<sup>†</sup> P. Papakonstantinou, Gamal Abbas, and P. D. Maguire  
*Nanotechnology & Integrated Bio-Engineering Centre (NIBEC),  
University of Ulster, Newtownabbey, BT37 0QB Northern Ireland, U.K.*

D. Bakirtzis

*Fire SERT, School of Built Environment, University of Ulster,  
Newtownabbey, BT37 0QB Northern Ireland, U.K.*

(Received 3 June 2008; Accepted 1 December 2008; Published 4 April 2009)

The Electron Cyclotron Resonance (ECR) plasma is a relatively new and scalable technique which opens up possibilities for a more environmentally friendly and rapid method of nanotube purification. We report a single step, dual purification and functionalisation technique using nitrogen-ECR plasma and compare results to those from standard RF plasma via Raman, Thermal Gravimetric Analysis (TGA), X-ray Photon spectroscopy (XPS) and static contact angle measurement. The purity of the nanotubes was evaluated by TGA which showed ~96% for the N-ECR treated and ~91% for the N-CCRF. Defects introduced by plasma exposure acted to functionalise the nanotubes by nitrogen attachment as evidenced by Raman, XPS and static contact angle measurements. The impact of nitrogen ion bombardment with two different plasma ion energies is fingerprinted by the defects induced in the nanotube matrix. [DOI: 10.1380/ejsnt.2009.337]

Keywords: Nanotubes; Electron cyclotron resonance (ECR); Functionalisation; Ion energy; Purification; X-Ray photoelectron spectroscopy

### I. INTRODUCTION

Single walled carbon nanotubes (SWCNT) offer many potential applications due to their unique structure and properties [1]. However the lack of high purity nanotubes poses a barrier to such developments. As-grown nanotubes contain high levels of impurities such as metal nanoparticles and amorphous carbon [2], the amount depending on the growth mechanism such as the arc discharge, laser ablation, catalytic chemical vapour deposition (CCVD), plasma enhanced chemical vapor deposition (PECVD) and others [3] and their purification remains a major challenge. The traditional chemical methods of purification rely on strong acid treatment which has limited efficacy. Plasma-based methods offer alternative purification routes whereby activated radicals and/or ion bombardment can decompose impurities into volatiles and simultaneously, depending on gas composition, modify the nanotube surface chemical composition to enable functional group attachments. Plasma processing has the particular advantage of avoiding the use, and subsequent disposal, of hazardous chemicals used in wet chemical methods. Various precursors, such as oxygen-argon mixtures [4, 5], hydrogen [6], fluorine, ammonia, nitrogen, H<sub>2</sub>O [7–9] or only oxygen [10] have been reported. Radio frequency (RF) generated plasmas are the standard method for surface modification in many disparate fields. Nitrogen is most extensively used to produce CN<sub>x</sub> nanotubes which are vital for a range of electronic and biological applications [11, 12].

In this work, a novel Electron Cyclotron Resonance (ECR) plasma process is investigated in order to obtain

both purification and functionalisation in a single step technique and results are compared with exposure to a standard capacitively coupled RF (CCRF) plasma system. The morphology, structural properties and purity of the untreated and plasma treated nanotubes have been investigated by Raman Spectroscopy and TGA. The surface reactivity after the nitrogen plasma treatment is demonstrated by the XPS and the contact angle measurements.

### II. EXPERIMENT

Arc discharge [13] produced single walled carbon nanotube (SWCNTs) from CarboLex Inc (U.S.A.), was used throughout this study. The SWCNT's (taken as powder) initial purity was evaluated by the thermo-gravimetric analysis (TGA). For the plasma treatment the samples were prepared by first dispersing the nanotubes in N-N; dimethylformamide (DMF) solution in the ratio 1:1, followed by ultra-sonication for 10 minutes and was finally drop dried on an *n*-type Si(100) wafer before being loaded into the ECR system for plasma treatment. The nitrogen plasma was generated using a 2.45 GHz ECR plasma source and the plasma power varied, under constant magnetic field conditions. The condition for maximum purification were achieved with a microwave power of 100 W at 0.2 mTorr. The CCRF nitrogen plasma was obtained for input powers that resulted in a DC self-bias of -100 V at 10 mTorr. These untreated (UT) and treated nanotubes (N-ECR and N-CCRF) were investigated using a high resolution x-ray photon spectroscopy (XPS), (Sci-enta ESCA300), equipped with a hemispherical energy analyser, Al K $\alpha$  x-ray source. The thermal analysis for the UT and plasma treated samples were carried out with Pyris 1 TGA analyzer (Perkin Elmer). The initial sample for test weighed 1 mg. The tests were performed under flowing nitrogen atmosphere at a temperature range between 90-900°C with a linear heating of 10°C/minute.

\*This paper was presented at the 14th International Conference on Solid Films and Surfaces (ICSFS-14), Trinity College Dublin, Ireland, 29 June - 4 July, 2008.

<sup>†</sup>Corresponding author: iyer-s@ulster.ac.uk

Raman spectra were measured using a 633 nm red laser in the back scattering mode. Static water contact angle measurements were obtained using the sessile drop method (Cam 200 optical contact angle meter).

### III. RESULTS AND DISCUSSION

#### A. Thermogravimetry Analysis (TGA)

Figure 1(a) shows the TGA of the untreated and treated samples while Fig. 1(b) shows the derivative of the TGA. For the UT case, the initial burn off temperature is  $<300^{\circ}\text{C}$  and this can be attributed to the soot amorphous carbon and soot associated with the nanotubes. The weight loss of the UT at  $900^{\circ}\text{C}$  is  $\sim 12.4\%$  which accounts for the metal catalyst and some metal nanoparticles encapsulated in carbon which, may not be completely burnt off. The N-ECR purified samples show two step weight losses, the first step occurring at  $360^{\circ}\text{C}$  while the second step at  $622^{\circ}\text{C}$ . The initial burn off at  $360^{\circ}\text{C}$  can be attributed to the gradual removal of soot and associated amorphous carbon. We have observed the initial burn off temperature for the nitrogen treated SWCNT is increased by  $>\sim 60^{\circ}\text{C}$  which can be due to the removal of soot and amorphous carbon partially by the ion bombardment. A second step at  $622^{\circ}\text{C}$  is due to the loss of  $-\text{OH}$  or  $-\text{COOH}$  functional groups [14] and oxidation of metal particles. The final weight loss for the N-ECR treated SWCNTs was  $\sim 96\%$  with the remaining 4% thought to contain remnant metal nanoparticle residues. Similar results were obtained for the CCRF treated nanotubes which showed  $\sim 91\%$  weight loss at  $1000^{\circ}\text{C}$ . Figure 1(b) represents the derivative of the TGA. Since the maxima,  $dW/dT$ , for the untreated nanotubes is broad, the exact SWCNT burn-off temperature cannot be determined and is estimated as  $\sim 585 \pm 5^{\circ}\text{C}$ . The  $dW/dT$  maximum is observed at  $636^{\circ}\text{C}$  which is the burn off temperature for the N-ECR treated nanotubes, an increase of  $50 \pm 5^{\circ}\text{C}$  compared to the untreated nanotubes. Nikolaev *et al.* [14] have attributed the increase in the oxidation temperature to the higher thermal stability of the nanotubes and in our case it therefore suggests the ECR plasma process does not result in significant damage. For the N-CCRF the  $dW/dT$  maxima is observed at  $520^{\circ}\text{C}$ , a decrease in the thermal stability compared to both the UT and the N-ECR treated samples, due possibly to oxygen uptake at active sites created by the nitrogen plasma, upon exposure to atmosphere. The potential difference between sample and plasma is much higher in the RFCC case ( $>100\text{V}$ ) compared to ECR (few volts) and hence ion bombardment is likely to be much more energetic and a possible source of extra defect generation as a source for active site oxygen uptake.

#### B. X-ray Photon Spectroscopy (XPS)

Figure 2(a) shows the wide energy scan (WES) XPS of the untreated and the plasma treated SWCNT. Figures 2(b), 2(c) and 2(d) represent the C 1s, N 1s and O 1s core levels of the same samples respectively. The intensity of carbon decreases and the peak broadens, after

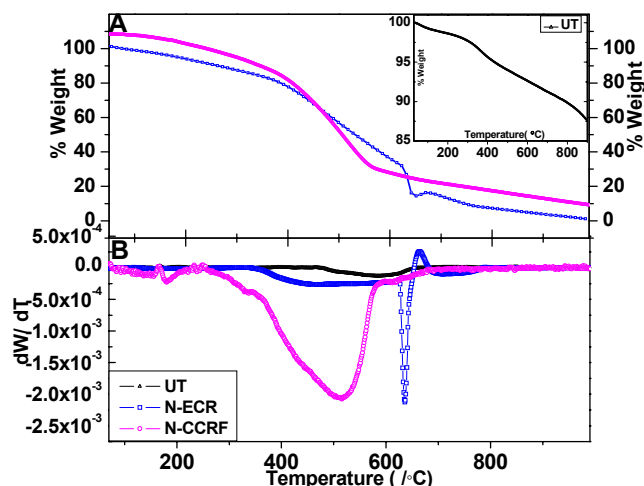


FIG. 1: (a) Thermal Gravimetric Analysis (TGA) curve. The inset represents the TGA of the untreated SWCNT. (b) The derivative of the TGA curves for the untreated and nitrogen plasma treated SWCNT.

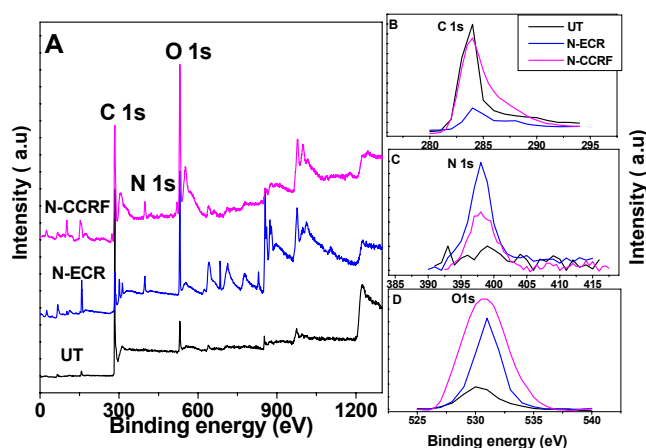


FIG. 2: (a) XPS survey spectra, measured at normal incidence ( $90^{\circ}$ ), UT (untreated), and plasma treated SWCNT. (b), (c), (d): The XPS spectra of the same samples at C 1s, N 1s and O 1s core levels respectively.

nitrogen plasma treatment indicating the removal of the amorphous carbon surrounding the metal particles and the nanotubes. In the WES for the untreated sample, no peaks related to the catalyst particle (nickel and yttrium) are observed, but these peaks are visible for the plasma treated samples. XPS, being a surface technique cannot probe catalyst particles which are embedded in the carbon but as this encapsulation is removed, the metal particles become exposed and their peaks get stronger. In the N-ECR treated sample the total metal concentration (at. % conc.) of nickel and yttrium is  $\sim 4\%$ , in agreement with the TGA (residue  $\sim 4\%$ ). The atomic concentration of nitrogen increases from 0.95 at. % to 13.10 at. %.

It has been shown [15] that the nitrogen substitutes the carbon in the planar, graphite like environment. Also Terrones *et al.* [16] have shown that both multiwall nanotubes and graphite, treated in a nitrogen atmosphere, are chemically reactive because of the pyridine like defects. The

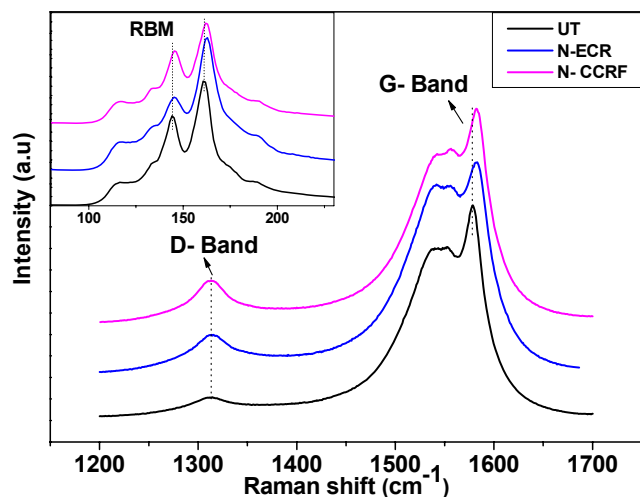


FIG. 3: shows the D and G band of the Untreated and nitrogen plasma treated SWCNT samples respectively. The inset shows the RBM for the same samples between of the frequency 100-250  $\text{cm}^{-1}$  respectively

increase in the nitrogen can be attributed to the substitution of the N in the carbon sheet, at the defect sites. There is a substantial increase in the oxygen concentration of the plasma treated nanotubes from 7.21 at. % (UT) to 40.26 at. % for the N-ECR treated SWCNT. The defects created by the plasma bombardment are highly reactive and can also chemisorb oxygen upon exposure to atmosphere [17] and also observed in our previous work [18] for vertically aligned nanotubes treated by nitrogen RF plasma. The nitrogen plasma creates not only nitrogen related defects but also leaves carbon dangling bonds that might act as the active sites for the oxygen adsorption. In the case of RF plasma the at. % conc. of oxygen is greater than that of nitrogen.

### C. RAMAN SPECTROSCOPY

Figure 3 shows the Raman spectra for the UT and the plasma purified single walled nanotubes where the D-peak is indicative of induced defects while the G-peak is associated with the tangential graphitic mode. The increase or decrease in the D to G intensity ratio ( $I_D/I_G$ ) can be used to indicate structural changes made to the nanotubes. The radial breathing mode (RBM) which is a signature of SWCNT [19] is observed in both the untreated and the N-plasma treated samples at the low wave number (100-200  $\text{cm}^{-1}$ ). There are five to six RBM observed at 116.4, 133.06, 144.13, 160.71, 173.9, 188.24  $\text{cm}^{-1}$  respectively. The diameters of the RBM, from  $d$  (nm) =  $248/\nu$  ( $\text{cm}^{-1}$ ) [20], range from 2.1nm to 1.3 nm. For the plasma treated samples the RBMs are up shifted and the peak at  $\sim 174$   $\text{cm}^{-1}$  disappears indicating the removal of smaller diameters. The G-band is double peaked with two components  $G^-$  and  $G^+$ . The  $G^-$  (1538  $\text{cm}^{-1}$ ) and  $G^+$  (1577.9  $\text{cm}^{-1}$ ) for the untreated SWCNT is up shifted to  $G^-$  (1540  $\text{cm}^{-1}$ ) and  $G^+$  (1580.5  $\text{cm}^{-1}$ ) and this is attributed to nitrogen chemisorption on the nanotube surface after the N-plasma treatment [21]. Since nitrogen can

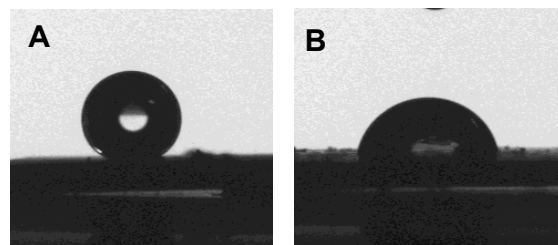


FIG. 4: (a) The static contact angle of the Untreated SWCNT and (b) the contact angle of the nitrogen plasma treated SWCNT.

easily accept an electron, it attaches to the active carbon in the graphitic sheets leading to co-valent side wall functionalisation. A similar observation is shown by Khare *et al.* with the SWCNT treated by ammonia microwave glow discharge plasma [8, 22]. A small intermediate D peak is observed at 1310  $\text{cm}^{-1}$  for the untreated single walled up shifted to 1313.6  $\text{cm}^{-1}$ .

The exposure of nanotube to the plasma has both physical and chemical effects. The chemical effect leads to chemical reaction between the nitrogen species and the nanotube surface creating functional groups and the physical effect of ion bombardment leads to the formation of defects [23, 24]. The up shift in the D and G peak can be attributed to the nitrogen functionalisation which takes place along with purification. The  $I_D/I_G$  for the UT SWCNT is 0.08 which increased to 0.17 for the N-ECR and to 0.28 for the N-CCRF treated nanotubes. An increase in the  $I_D/I_G$  ratio indicates enhanced surface defects, which can be due to the N chemisorption and consequent uptake of oxygen on the CNT surface leading to a high degree of functionalisation [25].

### D. CONTACT ANGLE MEASUREMENT

The change in the wettability of the nanotube surface by the nitrogen ion bombardment is obtained by static contact angle measurement. The nanotubes which are hydrophobic in nature are made hydrophilic by the functionalisation due to the nitrogen plasma. Figures 4(a) and 4(b) show contact angle of the untreated SWCNT and the nitrogen plasma treated nanotubes respectively. The contact angle, the angle between the surface of the nanotube and the water droplet for the UT was measured to be 108° and the angle for the plasma treated is 72.5°. The nanotubes that were untreated (raw) already possess some defects on the surface. The surface of the nanotubes is covered by active C atoms and C-C which are covalently bonded. The  $\text{N}_2$  introduced dissociates into 2[N] and initially reacts with the active C or the dangling C present, simultaneously breaking the C-C covalent bonds. Since the system is not an ultra high vacuum (UHV) there may be the presence of  $\text{O}_2$  from the air. By turning on the plasma the  $\text{O}_2$  immediately dissociates as  $\text{O}_2 = 2[\text{O}]$  and have a much higher tendency to react (as it is more electronegative than carbon) with the active C atoms on the surface walls of the SWCNT than the nitrogen which is allowed in to the chamber as the dissociation energy of

the oxygen is less than the dissociation energy of nitrogen [26].

#### IV. CONCLUSION

We have reported a novel, single step, plasma treatment using ECR plasma which results in side wall functionalisation and purification ( $\sim 96\%$ ), and is much simpler than the wet chemical treatment. Similar purification levels ( $\sim 91\%$ ) are also obtained using a standard RF plasma but at the cost of significantly higher defect generation. ECR plasma treatment has also been shown to simultaneously functionalize the nanotubes thus offering an efficient dual-purpose single step technique. Spectra from Raman

and XPS validate the functionalisation occurring at the defects created by the nitrogen plasma where nitrogen species irradiation enhances the chemical reactivity of the nanotube surface enabling the attachment of functional groups. The Raman showed an increase in the defects for the both ECR and CCRF. The difference in the level of defects between ECR and RF is considered due to the much higher ion bombardment energy in the latter. This shows the energy of the ion bombardment is an important factor in the defect generation and increased surface activity of the nanotubes. Reducing the ion energy is possible in the RF case but at the cost of much lower species (radical and ionic) flux and more detailed investigation is required to elaborate the purification-functionalisation dependence on ion energy-flux and neutral flux densities.

- 
- [1] S. Iijima, *Nature* **354**, 56 (1991).  
 [2] K. Hata, D. N. Futaba, K. Mizuno, T. Namai, M. Yumura, and S. Iijima, *Science* **306**, 1362 (2004).  
 [3] K. Tanaka, T. Yamabe, and K. Fukui (Eds.), *The Science and Technology of Carbon Nanotubes* (Elsevier, 1999).  
 [4] R. C. Haddon, J. Sippel, A. G. Rinzler, and F. Papadimitrakopoulos, *Mater. Res. Soc. Bull.* **29**, 252 (2004).  
 [5] M. Ohkohchi, X. Zhao, S. Inoue, and Y. Ando, *Jpn. J. Appl. Phys.* **43**, 8365 (2004).  
 [6] S. R. C. Vivekchand, A. Govindaraj, M. M. Seikh, and C. N. R. Rao, *J. Phys. Chem. B* **108**, 6935 (2004).  
 [7] A. Felten, C. Bittencourt, J. J. Pireaux, G. Van Lier, and J. C. Charlier, *J. Appl. Phys.* **98**, 074308 (2005).  
 [8] B. N. Khare, P. Wilhite, R. C. Quinn, B. Chen, R. H. Schingler, B. Tran, H. Imanaka, C. R. So, C. W. Bauschlicher Jr., and M. Meyyappan, *J. Phys. Chem. B* **108**, 8166 (2004).  
 [9] S. Huang and L. Dai, *J. Phys. Chem. B* **106**, 3543 (2002).  
 [10] D. S. Rawat, N. Taylor, S. Talapatra, S. K. Dhali, P. M. Ajayan, and A. D. Migone, *Phys. Rev. B* **74**, 113403 (2006).  
 [11] K. Xiao, Y. Liu, P. Hu, G. Yu, Y. Sun, and D. Zhu, *J. Am. Chem. Soc.* **127**, 8614 (2005).  
 [12] S. S. Roy, P. Papakonstantinou, T. I. T. Okpalugo, and H. Murphy, *J. Appl. Phys.* **100**, 053703 (2006).  
 [13] A. R. Harutyunyan, B. K. Pradhan, J. Chang, G. Chen, and P. C. Eklund, *J. Phys. Chem. B* **106**, 8671 (2002).  
 [14] P. Nikolaev, O. Gorelik, R. K. Allada, E. Sosa, S. Arepalli, and L. Yowell, *J. Phys. Chem. C* **111**, 17678 (2007).  
 [15] R. Droppa Jr., P. Hammer, A. C. M. Carvalho, M. C. Dos Santos, and F. Alvarez, *J. Non-Cryst. Solids* **299-302**, 874 (2002).  
 [16] M. Terrones, *International Mater. Rev.* **49**, 325 (2004).  
 [17] S. M. Lee, Y. H. Lee, Y. G. Hwang, J. R. Hahn, and H. Kang, *Phys. Rev. Lett.* **82**, 217 (1999).  
 [18] G. Abbas, P. Papakonstantinou, G. R. S. Iyer, I. W. Kirkman, and L. C. Chen, *Phys. Rev. B* **75**, 195429 (2007).  
 [19] M. S. Dresselhaus, G. Dresselhaus, R. Saito, and A. Jorio, *Phys. Rep.* **409**, 47 (2005).  
 [20] S. Bandow, S. Asaka, Y. Saito, A. M. Rao, L. Grigorian, E. Richter, and P. C. Eklund, *Phys. Rev. Lett.* **80**, 3779 (1998).  
 [21] B. Khare, P. Wilhite, B. Tran, E. Teixeira, K. Fresquez, D. N. Mvondo, C. Bauschlicher Jr., and M. Meyyappan, *J. Phys. Chem. B* **109**, 23466 (2005).  
 [22] J. L. Stevens, V. U. Kini, A. Y. Huang, I. W. Chiang, G. A. Derrien, V. N. Khabashesku, and J. L. Margrave, in *NanoTech 2003*, 23-27 Feb. 2003 (Computational Publications, San Francisco, CA, USA, 2003).  
 [23] N. Chakrapani, S. Curran, B. Wei, P. M. Ajayan, A. Carrillo, and R. S. Kane, *J. Mater. Res.* **18**, 2515 (2003).  
 [24] H. Kuzmany, A. Kukovecz, F. Simon, M. Holzweber, C. Kramberger, and T. Pichler, *Synth. Metals* **141**, 113 (2004).  
 [25] Y. H. Yan, M. B. Chan-Park, Q. Zhou, C. M. Li, and C. Y. Yue, *Appl. Phys. Lett.* **87**, 213101 (2005).  
 [26] Z. N. Utegulov, D. B. Mast, P. He, D. Shi, and R. F. Gilland, *J. Appl. Phys.* **97**, 104324 (2005).